JMEPEG
https://doi.org/10.1007/s11665-024-09445-z

1059-9495/$19.00

ORIGINAL RESEARCH ARTICLE

The Role of Microstructure in the Gradient of Tensile Properties through Thickness in 7449 Aluminium Alloy Thick Plate

J.A. Heredero, J. Medina, J.M. Antoranz, and P. Adeva

Submitted: 19 July 2023 / Revised: 20 January 2024 / Accepted: 26 February 2024

In this article, the yield strength, tensile strength, and the microstructure of the wrought aluminium alloy 7449 rolled thick plate have been studied through thickness under different temper conditions. For all heat treatments, it has been proven that the yield strength and tensile strength values increase from the surface to the centre. The largest difference between the centre and the surface, in both properties, occurs in the case of a sample aged at room temperature for 120 h (TTA temper). The sample artificially aged at 120 °C for 24 h (TTB temper) shows the best strength-gradient relationship of the tensile properties through the thickness. Metallographic characterisation carried out by optical and scanning electron microscopy shows much finer elongated grains in the region near the surface of the plate than in the centre, with incipient recrystallisation in the area near the surface. In addition, electron backscattered diffraction technique, used for micro-texture analysis, has proven the presence of a gradient of crystallography texture in the plate. This explains the yield strength gradient, since the rate of change of the Taylor factor through thickness correlates with the rate of the change of yield strength in the longitudinal direction for the samples studied.

Keywords 7449 aluminium alloy, micro-texture, Taylor factor, yield strength

1. Introduction

The AA7449 wrought alloy is an age-hardened Al-Zn-Mg-Cu alloy, developed by Pechiney in France during the 1990s and characterised by its high Zn content. It is an alloy for aeronautical applications. The alloy AA7449 is usually supplied in plate form of different thicknesses with two commercial over-aged heat treatments: T7651 (proprietary ageing treatment, more over-aged) and T7951 (proprietary ageing treatment slightly over-aged) (Ref 1-4). Interest in this alloy, especially used in aircraft wings, is due to the fact that it reaches very high resistance levels. However, it is known to be very susceptible to various types of corrosion, so they often have to be used in an over-aged state (e.g. T7651) for better stress corrosion resistance at the cost of slightly lower yield strength compared to T651 peak-aged temper.

Nevertheless, aluminium alloy plates of the 7XXX series have been found to exhibit inhomogeneous mechanical properties throughout thickness (Ref 5-11). For this reason, researchers have dedicated their efforts to studying the reasons for this behaviour with different results. This is the case of the work performed by Schloth et al. (Ref 5) where using a model to simulate the variation in yield strength by thickness on a 75-mm-thick plate of the 7449 aluminium alloy under T4 condition (solution heat treated and natural ageing) showed that the highest yield strength of 288 MPa was found 1.5 mm below the surface and the lowest value of 218 MPa corresponded to the centre of the plate. Other experimental works have shown different results from the above-mentioned model. For example, the work of Chakrabarti et al. (Ref 6) with a 7050 T74 aluminium alloy in a 50 mm thick plate showed that the yield strength in the rolling direction adopted a 'W-shape', reaching its maximum value at the centre of the plate. Chen et al. (Ref 7) found similar behaviour with a 19-mm-thick 7055 aluminium alloy plate in T7751 condition, where the yield strength increased from 576 MPa in the surface to 602 MPa in the centre of the plate. Li et al. (Ref 8) analysed the effect of different solution treatments on the mechanical properties of 7A65 superthick hot-rolled plates made of aluminium alloy (120-mm thick). The mechanical properties of the plate after the single-stage solid exhibit higher strength and lower elongation at H/4 (1/4 thickness) than at H/2 (1/2 thickness). Recent work such as that carried out by Wang et al. (Ref 9) also shows a variation in mechanical properties through thickness on a superthick plate (80 mm) of the 7B50 aluminium alloy (Al-Zn-Mg-Cu). There is a marked difference in engineering strain (%) between the surface (higher %) and the centre (lower %). This pattern, maximum yield strength in the centre and minimum value at the surface, has also been observed by Vasudevan et al. (Ref 10) in a thin plate thickness (12 mm) in 2029 alloy (Al-Li-Cu-Zr) alloy under the temper condition T8E41 (solution treated, stretched, and aged). However, in the work of Salazar-Guapuriche et al. (Ref 11) the hardness was also measured by thickness on a plate of 157 mm of 7010-

J.A. Heredero and **J.M. Antoranz**, Department of Aerospace Materials and Production, Escuela Técnica Superior de Ingeniería Aeronáutica y del Espacio, Universidad Politécnica de Madrid, Pza del Cardenal Cisneros, 3, 28040 Madrid, Spain; and **J. Medina** and **P. Adeva**, Department of Physical Metallurgy, CSIC, Avenida Gregorio del Amo, 8, 28040 Madrid, Spain. Contact e-mail: joseantonio.heredero@upm.es.

Published online: 15 April 2024

T7651 alloy showing the maximum value near the surface and the minimum in the centre of the plate. Electrical conductivity showed the opposite behaviour, reaching the maximum value in the centre and the minimum near the surface.

There are several factors, or a combination of them, responsible for this behaviour, such as a decrease in the rate of quenching from the surface to the centre of the plate, an inhomogeneity of the alloying elements through the thickness of the alloy, etc. (Ref 6). Plastic deformation induced by rolling operations increases mechanical properties, particularly yield strength and tensile strength. Furthermore, the plastic deformation induced by the application of stress relief varies in intensity along the thickness, being greater in areas near the surface than in the centre of the plate (Ref 4, 12, 13). In areas where plastic deformation is more intense and, as a consequence, the effect of directionality is more evident, the tensile properties are greater (Ref 14). However, differences in the microstructure and texture of materials through thickness can be very important in contributing to producing heterogeneity in mechanical properties, an effect that is even more important with increasing thickness. Although historically the major cause of the yield strength gradient has been attributed to the crystallographic texture, it was demonstrated in thin sheets of the AI-Li-Cu-Zr alloy that because the texture was uniform throughout the thickness, the yield strength varied with angle of the tensile axis to the rolling direction. However, in the case of thick plates, the crystallographic texture was only part of the contribution to the variation of the yield strength (Ref 8-10).

To clarify which factors contribute to the generation of gradients in both yield strength and tensile strength through the thickness of 54-mm-thick aluminium alloy 7449 plate under different ageing conditions, full microstructural characterisation has been carried out using optical metallographic microscopy, scanning electron microscopy and microanalysis, and electron backscattered diffraction (EBSD) for micro-texture analysis.

2. Experimental Procedure

The chemical composition of the alloy 7449, provided by the supplier and studied in the present work, is shown in Table 1. It was provided as a thick plate with dimensions 1560 mm in longitudinal direction (RD) × 765 mm in transverse direction (TD) × 54 mm in normal direction (ND) under the T7651 condition.

The blocks dimensions, prior the heat treatments, were 155 mm × 60 mm × 54 mm. These blocks were extracted from the plate. The different heat treatments performed are shown in Table 2.

All heat treatments performed in this investigation have been solution-treated heating (*W*) to 468 °C for 3 h in a REVSAL 430 salt bath, followed by quenching with cold water at room temperature.

The microstructural characterisation of the alloy under the different conditions was performed by optical microscopy and scanning electron microscopy (SEM) using a HITACHI S-3400N equipped with an energy dispersion spectroscopy (EDS) system. The samples were prepared by conventional mechanical polishing followed by etching with Keller's reagent (95 vol.% H_2O + 2.5 vol.% HNO_3 + 1.5 vol.% HCl + 1 vol.% HF). The samples were prepared in the RD, TD, and ND directions. In addition, in the RD direction, two through-thickness samples were prepared for observation, one near the surface and the other near the centre. Micro-texture analysis of T7651 and TTB temper was carried out using the electron backscattered diffraction (EBSD) technique attached to the SEM Jeol JSM 6500F equipment, using Channel 5 EBSD software to analyse the data. The samples have a cubic symmetry, where the reference directions are the rolling direction (RD), the transverse direction (TD), and the normal direction (ND). Orientation image maps (OIM) were taken in the RD-TD section using a step size of 1.5 μm. The black lines represent the high-angle grain boundaries ($> 10°$) while the white lines correspond to the low-angle grain boundaries ($> 2°$). The samples were prepared by electropolishing.

Tensile tests were carried out with a universal testing machine MTS 810, with controlled displacement and a strain rate of 1 mm/min. according to the UNE-EN-ISO 6892-1:2009 standard (Ref 15). Round samples of total length L = 155 mm with an internal calibrated diameter d = 8 mm extracted from the plate with the longest dimension parallel to the longitudinal direction (RD) were machined. Seven cylindrical specimens (specimen #1 to specimen #7) were extracted equidistantly through the thickness (ND), in such a way that specimen #4 corresponds to the centre of the plate thickness. Hardness measurements were also made by thickness in samples with temper conditions T7651, TTB, and TTC. Macro-Vickers hardness was used with 30 kg according to the standard ISO 6507-1.

3. Results and Discussion

3.1 Microstructural Characterisation

Figure 1 shows optical micrographs of the 7449 alloy in the received condition (T7651) in the three metallurgical directions: RD, TD, and ND, respectively, and located at ¼ of the plate thickness. The microstructures in the RD and TD directions are very similar.

The grain structure, in Fig. 1, is the typical and expected microstructure of rolled and heat treated alloys characterised by elongated grains in conjunction with recrystallised grains (Ref 3, 16-18). To verify the microstructural homogeneity through the thickness of the plate, samples near the surface and from the middle of the plate were observed, in the RD direction, by SEM microscopy. Figure 2 shows those grain structure.

Table 1 Chemical composition of 7449 experimental alloy (wt.%)

Zn	Mg	Cu	Mn	Fe	Si	Ni	Zr	Cr	Ti	Al
8.40	2.10	1.80	0.05	0.06	0.03	0.001	0.11	0.055	0.02	87.37

Table 2 Thermal heat treatments applied to the 7449 aluminium alloy

Heat treatment denomination	Description
W (solution)	Heated 468 °C 3 h + water quenching to room temperature
T7651 (as received condition)	Proprietary artificial ageing (pre-strained and over-aged)
T73[a]	Solution + 25 °C for 72 h + 121 °C for 24 h + 166 °C for 17 h
TTA[b]	Solution + natural ageing for 120 h
TTB	Solution + 120 °C for 24 h
TTC	T7651 + 160 °C for 8 h

[a]Heat treatment according to AMS 2772C for aluminium alloys 7049 and 7149.
[b]Unstable ageing at room temperature.

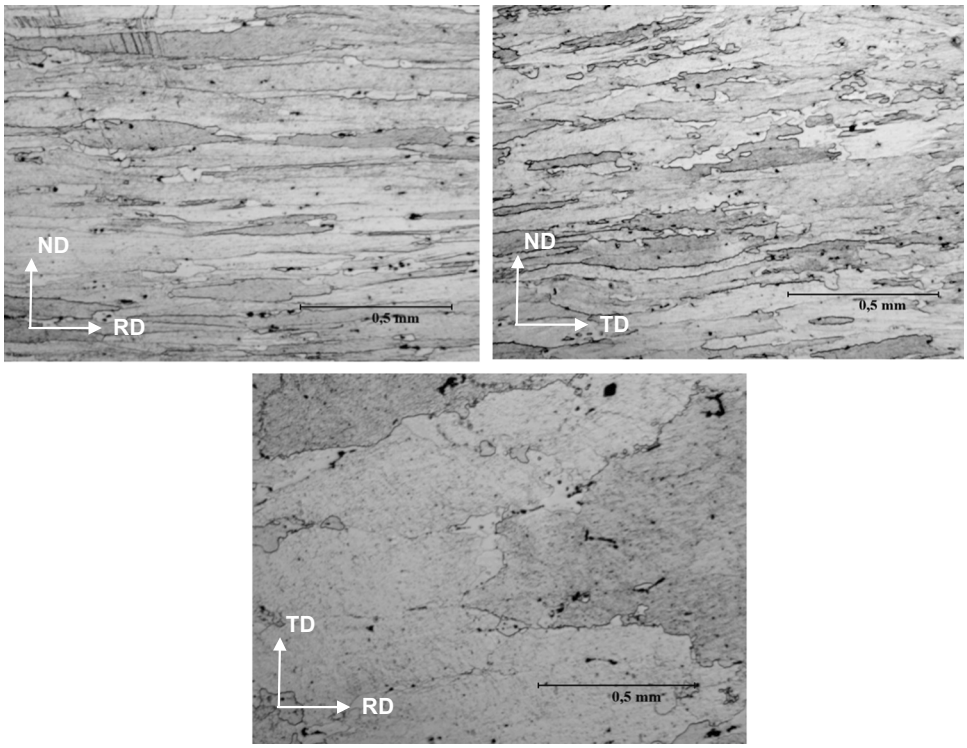

Fig. 1 Grain structure of the 7449 alloy in the T7651 temper obtained in the three metallurgical directions of the plate at ¼ of the plate thickness

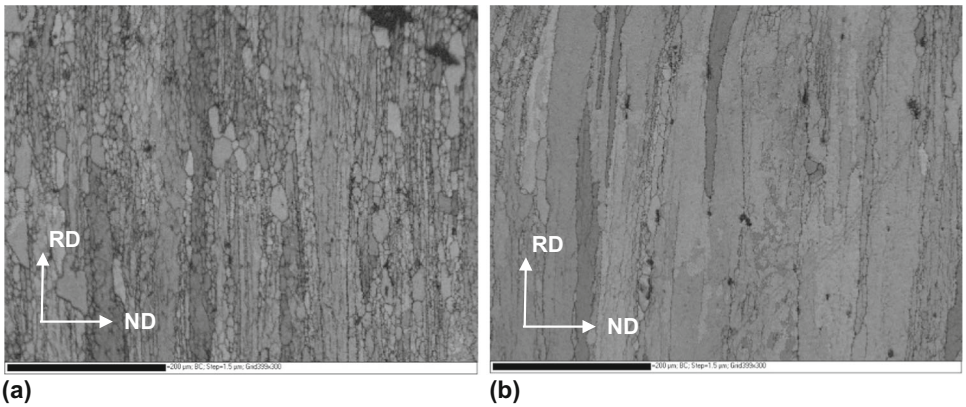

Fig. 2 SEM images of the grain structure in the RD direction: (a) near surface and (b) in the centre

According to the micrographs, both samples show elongated grains due to the rolling process. However, the sample close to (Fig. 2a) shows finer grains than those in the centre of the plate (Fig. 2b). This fact, as well as the presence of very fine equiaxed grains, indicates that partial recrystallisation occurred during the rolling operation. The degree of recrystallisation decreases from the surface to the middle of the plate. The same conclusion is reached in Ref 9. It is well known that a high degree of recrystallisation can significantly decrease the tensile properties of wrought Al 7xxx alloys. Therefore, it is necessary to control this process. The presence of dispersoid particles and alloying with zirconium are ways to inhibit the recrystallisation process (Ref 19). It is also very important to use the lowest solution temperature for the dissolution of the constituent particles to slow the recrystallisation process. Solution time and temperature are two parameters that should be kept as low as possible but achieving maximum dissolution of soluble particles at the same time, to maximise mechanical strength, toughness, and corrosion resistance (Ref 20, 21).

Second-phase particles are always present in an aluminium alloy. To confirm their presence, the backscattered electron images, in Fig. 3, show these particles through the thickness in the rolling direction (RD) for the received condition (T7651). Both micrographs show, in addition to the matrix, two different phases that can be distinguished by their morphology and contrast.

The bright particles, consisting of heavy elements, as characterised by ESD below, are coarse and polygonal in shape. The dark particles that correspond to a light phase are smaller and more rounded. These phases have been identified by other authors in the 7050 aluminium alloy (Ref 18, 22, 23). The metallographically images prepared through thickness appear to show a higher amount of second-phase particles in the region close to the surface than in the interior of the plate, as shown in Fig. 3 if images (a) and (b) are compared. To check whether this observation is correct, eight different fields were analysed in a longitudinal direction from the surface to the centre of the plate. The results indicate that in all fields, the percentages of the occupied area (with respect to the total area of the analysed field) of bright particles are higher than those of dark particles, as shown in Fig. 4.

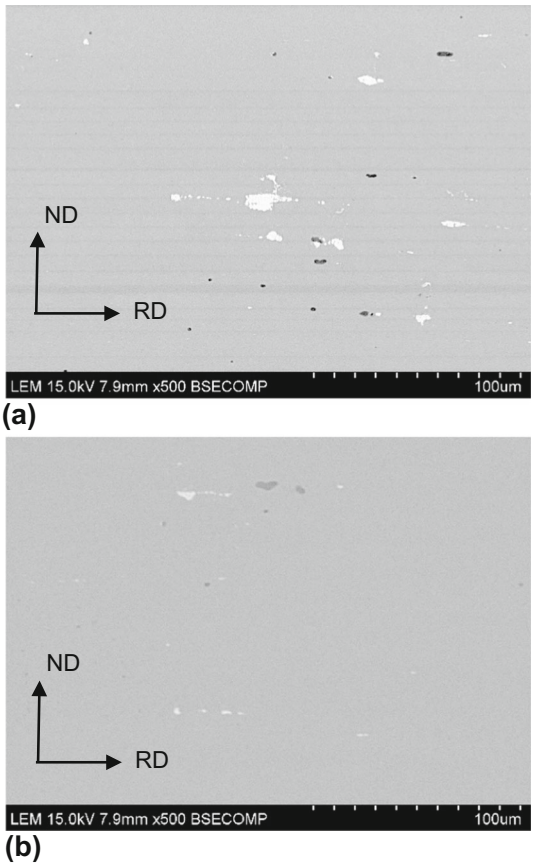

Fig. 3 Backscattered electron image of the T7651 sample in RD direction: (a) close to the surface and (b) in the middle

A detail of the bright and dark particles in one of the fields analysed near the surface is shown in Fig. 5(a) for the TTA temper and (b) for the T7651 heat treatment. Figure 5(b), with higher magnification, shows the polygonal shape of the bright particles versus the globular and more rounded shape of the dark particles. The fact that these phases are present in any ageing condition indicates that they are insoluble during solution treatment.

The microanalysis performed in the matrix and the phases are shown in the three spectra and in the table of Fig. 6. It is clear that the bright phase is a Fe, Cu-rich phase, probably Al_7Cu_2Fe, while the dark phase is an Mg, Si-rich phase, probably Mg_2Si. The same types of intermetallic phases are found in Ref 8 and 18. The presence of Cu and Fe in the bright phase gives it hardness and brittleness. This is the main reason these particles are fragmented. The matrix spectrum shows only the major elements, such as Al, Mg, Cu, and Zn.

3.2 Mechanical Properties

Tensile tests were performed on specimens machined through the thickness of the plate as described in the experimental part. The yield strength (0.2%) and tensile strength values for all heat treatments are shown in Table 3.

The variation of both properties as a function of the thickness of the plate is presented in Fig. 7.

All samples show similar behaviour, that is, lower values of both properties at the surface than in the middle of the plate, although in some samples the difference is small. From Fig. 7, it can be deduced that the TTB sample, artificially aged at the lowest temperature, without considering the natural aged sample, exhibits the highest values of mechanical strength, as expected according to the theory of age hardening. However, for the TTA sample, the measured yield strength values are the lowest. Since the solution treatment was the same for all samples, it can be assumed that the sample aged at room temperature has not yet reached the peak strength.

The percentages of variation of both properties (yield strength and tensile strength) between the centre and near the surface of the plate are presented in Fig. 8. Specimen #4 corresponds to the values obtained in the centre of the plate. In the case of the near-surface area, the average values between specimens #1 and #7 have been considered. This figure allows us to see which ageing treatment gives the alloy plate the most homogeneous mechanical properties throughout the plate. In this study, it can be concluded that the T73 sample is the most homogeneous, although at the cost of losing mechanical properties.

It is worth highlighting the case of the TTA sample, since it exhibits the largest difference in mechanical properties between the surface and the centre of the plate and, at the same time, has

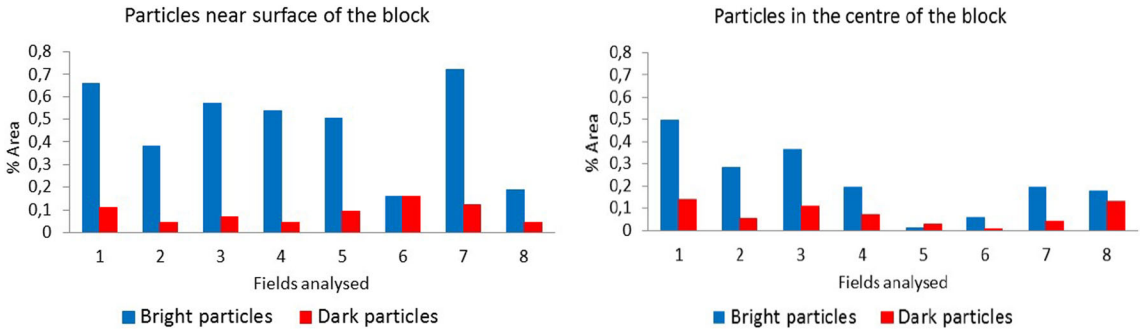

Fig. 4 Percentage of the area occupied by bright and dark particles near surface (left) and in the centre (right) in the T7651 sample

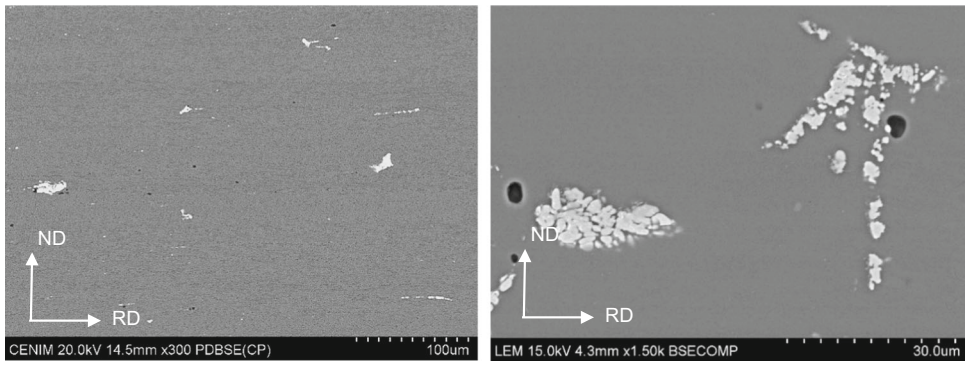

Fig. 5 Backscattered electron image of the intermetallic phases present in 7449 alloy: (a) TTA temper and (b) T7651 temper and detail at higher magnification of intermetallic phases

the lowest strength values. Therefore, this ageing treatment is ineffective in providing the alloy with the mechanical strength required for aeronautical applications. On the other hand, the TTB sample exhibits the best ratio strength-gradient of mechanical properties through the thickness. The permanence of the alloy at temperatures above room temperature leads to the precipitation of more stable phases, as opposed to what happens with the TTA treatment, reducing the percentage variation of the tensile stress and yield strength.

Variation in Vickers hardness through the plate thickness was also measured in the T7651, TTB, and TTC samples. The results are shown in Fig. 9. These graphs show a variation of hardness opposite to that shown by the yield strength and the tensile strength in such a way that a decrease in hardness is observed from the surface to the centre. Considering that the amount of intermetallic particles is higher near the surface than in the centre of the plate and the grain size is finer on the surface than in the centre, as shown in Fig. 2, it is possible to explain this hardness variation. These results agree with those obtained for the Al 7010 alloy in the study by Salazar-Guapuriche et al. (Ref 7). However, it should be noted that the hardness of the samples follows the same order as in the case of the tensile parameters. The hardness decreases in the order TTB, T7651, and TTC.

3.3 Micro-texture Characterisation

The micro-texture has been evaluated under the received condition (T7651) and in the heat treated TTB samples. The samples have been considered in three different areas through the thickness of the thick plate corresponding to the position of the tensile test specimens #1, #3, and #4. Only the positions of the tensile test specimens #1 (near the surface) and #4 (centre) designed as 1 and 4, respectively, are plotted.

Figure 10 shows the orientation image maps (OIM) and the {1 1 1} pole figures of the T7651 and TTB samples, together with the orientation colour key triangle. It can be clearly seen that all the coarser grains are elongated along the rolling direction because of the rolling process of the starting material. In the area close to the surface, the grains appear more flattened, which is consistent with the fact that the laminated material undergoes greater deformation in the near-surface area than in the inside area. The near-surface OIM images (Fig. 10a, b, c) show a small volume fraction of fine equiaxed high-angle grains, indicating incipient recrystallisation, in agreement with that previously mentioned in Fig. 2. A high density of low-angle grain boundaries (white lines) is also observed within the coarse grains, meaning that there was sufficient stored energy in these highly deformed grains to give rise to the recovery process.

During the recovery process, the dislocations are grouped together to form low-angle boundaries that draw small grains within the coarse ones. With the recrystallisation process, more dislocations are removed, and small equiaxed high-angle grains have been generated as can be seen in Fig. 10(a) and (c). This is in accordance with the pole figures in Fig. 10(b), (c), and (d). The pole figures close to the surface {1 1 1} show a softened texture in samples T7651-1 and TTB-1 with an intensity of 5.95 and 5.79, respectively, due to the partial recrystallisation without preferential orientation produced in the near-surface area. However, the areas close to the centre (Fig. 10e, f, g)

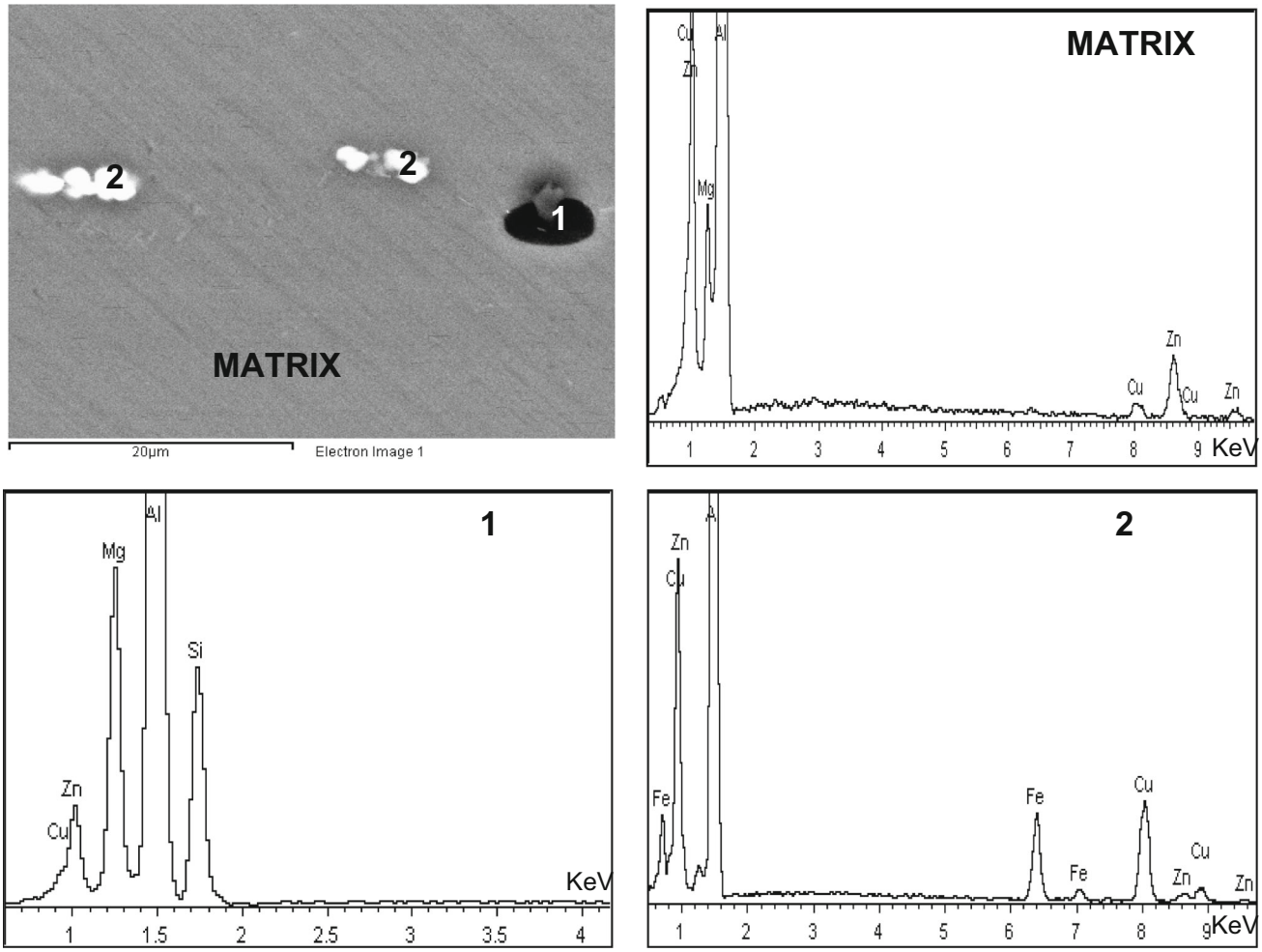

Spectrum/at. %	Mg	Si	Fe	Cu	Zn	Al
Matrix	2.20	0.07	0.14	0.79	4.05	93.03
Spectrum 1	12.60	19.67	0.02	0.65	2.77	64.29
Spectrum 2	1.10	0.05	6.32	13.02	1.23	78.28

Fig. 6 Results of the microanalysis of the phases present under the 7449 alloy in any temper condition. EDS spectra and chemical composition in at.%

Table 3 Tensile properties of the 7449 alloy in different temper conditions

	Yield strength (0.2%), MPa		Tensile strength, MPa	
Heat treatment denomination	**Centre[a]**	**External[b]**	**Centre[a]**	**External[b]**
T7651 (as received condition)	578	530	616	550
T73	470	443	514	481
TTA	380	314	545	474
TTB	596	540	652	606
TTC	518	488	569	522

Longitudinal direction (RD).
[a]Value obtained for the specimen #4 located in the centre of the plate.
[b]Average values of specimens #1 and #7.

present a lower density of low-angle grain boundaries within the coarse grains. Since the deformation in this area is lower than in the area close to the surface, the energy accumulated inside the coarse grains is lower and the recovery process is not so evident. These zones, in addition, exhibit a lower amount of recrystallised grains which leads to a more pronounced texture,

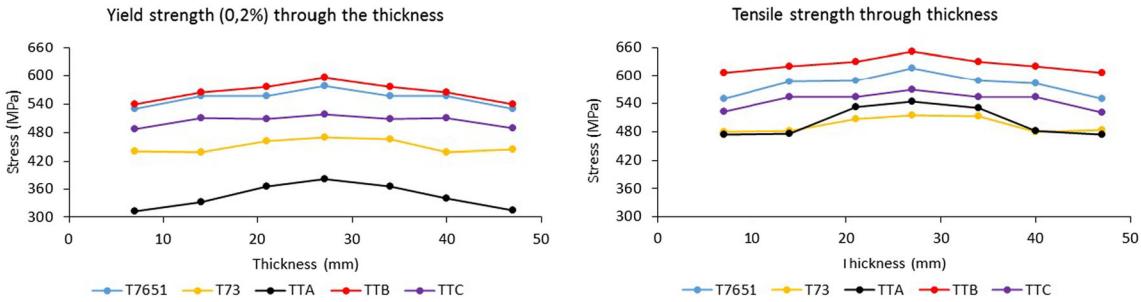

Fig. 7 Evolution of the yield strength (0.2%) (left) and tensile strength (right) through the thickness in RD direction

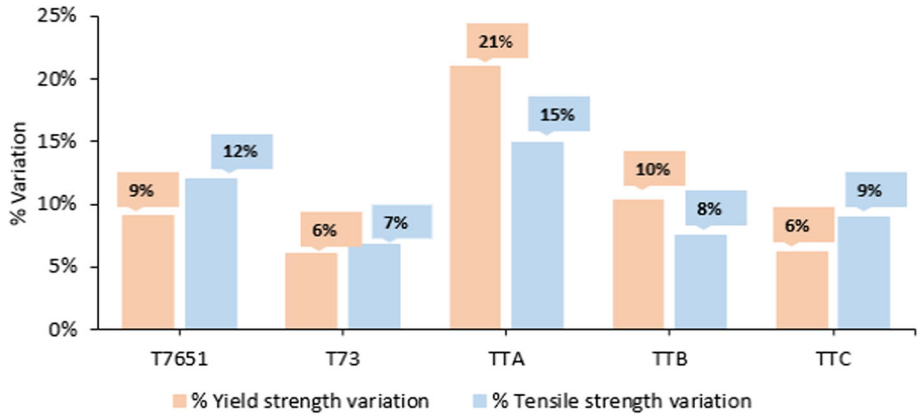

Fig. 8 Variation of the yield strength and tensile strength between the surface and the centre of the plate for all samples tested

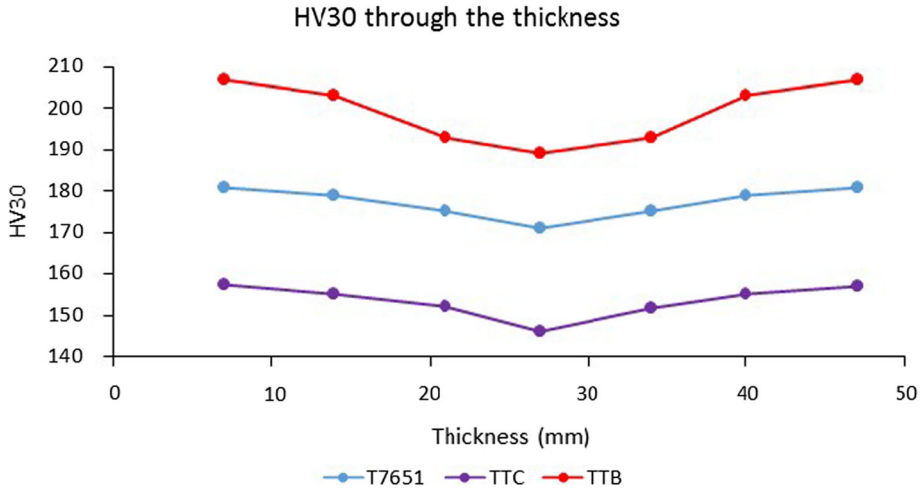

Fig. 9 Variation in HV30 hardness through the thickness in RD direction

as indicated by the pole figures (Fig. 10f, g, h) where the intensity increases to values of 11.58 and 17.48, respectively. It must be considered that the images taken in the centre contain fewer grains than the images taken close to the surface, which is logical because these grains are coarser. In addition, it should be noted that micro-texture is a local measure, and therefore, only a preferred texture can be stated.

To evaluate whether the variation of the texture through the thickness contributes to facilitate or hinder the {111} slip system in the course of deformation during tensile tests, the distribution maps of the Schmid factor (SF) {111} ⟨110⟩ along the RD (which is parallel to the load direction) were calculated.

Figure 11(a), (b), (c), and (d) shows the SF distribution maps with the corresponding histograms only for the positions near the surface (designated as 1) and in the centre (designated as 4). Dark colours correspond to Schmid factors closer to zero, while lighter colours match to values close to 0.5. Although there is no marked difference between the two regions for both samples, it can be observed how the SF values tend to be closer to 0.5 in the area near the surface (Fig. 11a, b), indicating a favourable orientation for the {111} slip system. Recrystallised grains are randomly oriented, and this contributes to achieved SF values closer to 0.5. On the contrary, in the area near the centre of thickness (Fig. 11c, d) the histogram changes

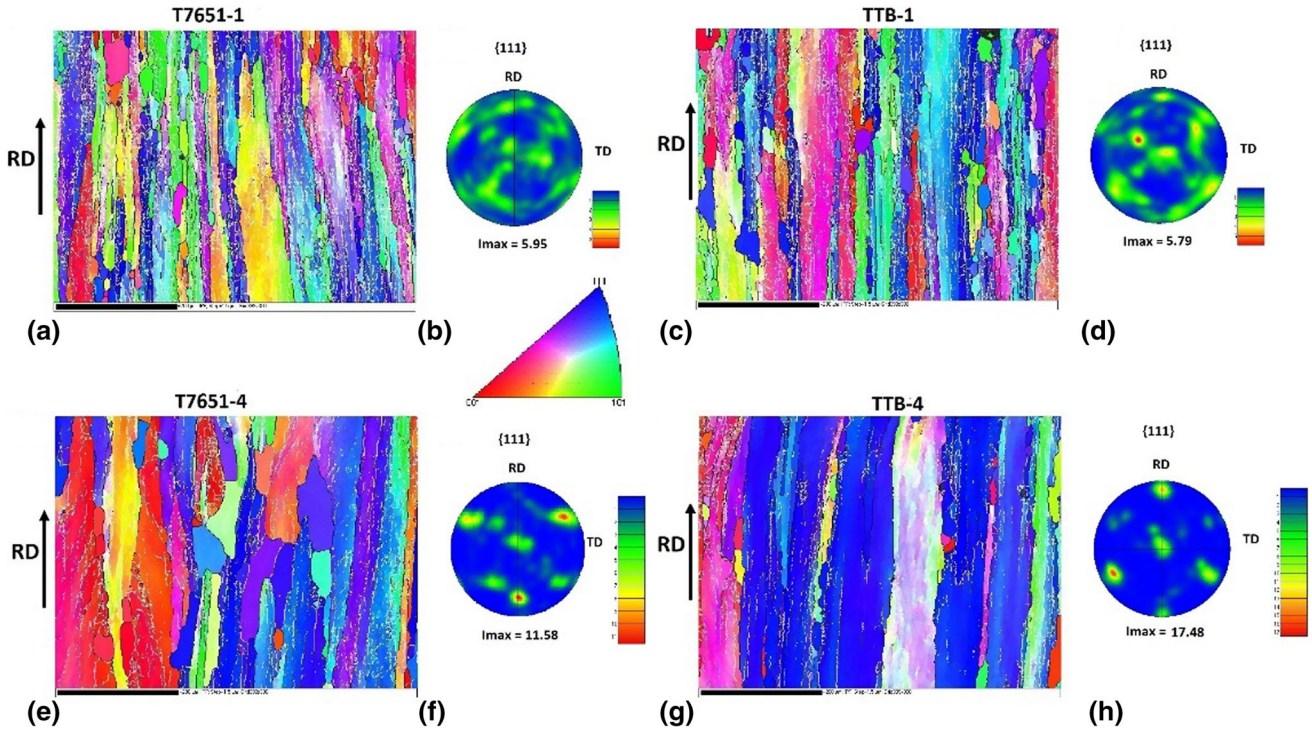

Fig. 10 Orientation Image Maps (OIM) and {1 1 1} pole figures of the T7651 sample (a, b) near surface and (e, f) in the centre, and the TTB sample (c, d) near surface and (g, h) in the centre, respectively

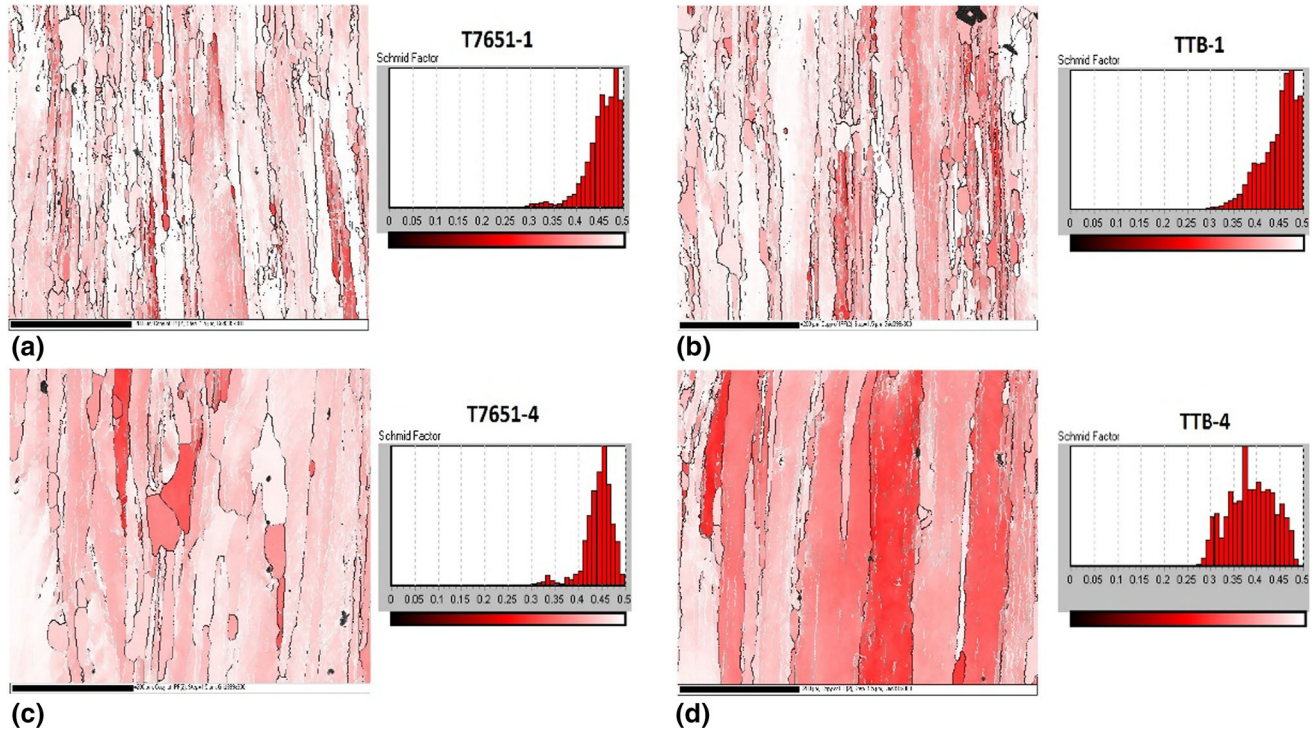

Fig. 11 {111} ⟨110⟩ Schmid factor distribution maps along RD of the T7651 sample (a) near surface and (c) in the centre, and the TTB sample (b) near surface and (d) in the centre

to lower values (dark red grains in the SF distribution maps) indicating that during the tensile test these grains offer higher slip resistance, which contributes to increase the yield strength of the material.

Based on the Schmid factor values extracted from the histograms in Fig. 11 and the position histogram corresponding to test specimen #3 (not shown in Fig. 11), the Taylor factor

Table 4 Schmid and Taylor factors in each analysed location

Location	Schmid factor	Taylor factor
T7651-1	0.50	2.02
T7651-3	0.46	2.20
T7651-3	0.43	2.33
TTB-1	0.46	2.17
TTB-3	0.41	2.44
TTB-4	0.39	2.60

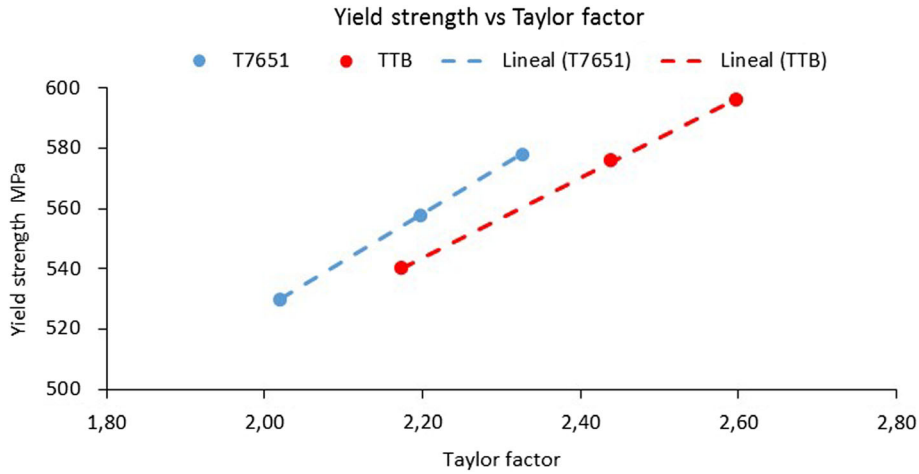

Fig. 12 Yield Strength evolution vs. Taylor Factor for the analysed locations

was estimated (simply by calculating the inverse of the Schmid factor) as shown in Table 4.

Since in a polycrystalline metal, the yield strength is related to the critical resolved shear stress (CRSS) by the following expression (Ref 24):

$$\sigma_y = \Delta\sigma_{gb} + M\tau_{tot} \quad \text{(Eq 1)}$$

where σ_y is the macroscopy yield strength, $\Delta\sigma_{gb}$ is the strength due to grain shape, M is the Taylor factor that depends on the texture and the orientation of the tensile axis respect the main axis of the specimen, and τ_{tot} is the CRSS of the grains. Therefore, to quantify whether the gradient in the crystallography texture alone can explain the variation of yield strength, the change of the Taylor factor versus the change of the yield strength in the longitudinal direction, through the thickness and for the two temper conditions analysed is plotted. Fig. 12 shows this rate of change.

In Fig. 12, the rate of change of the Taylor factor through thickness correlates with the rate of change of yield strength in the longitudinal direction for the treatments analysed. This means that the crystallographic texture gradient through the thickness in the longitudinal direction also explains the variation of the observed yield strength in the longitudinal direction. Furthermore, according to Ref 24 for typical rolling textures, the average Taylor factor values are about 15% higher than those obtained for recrystallisation textures. This statement is consistent with the results obtained in this study. The Taylor factor between the surface and the centre is 15% for T7651 and 19.5% for TTB following the results of Table 4 above. The intensity of the texture obtained for the TTB treatment in the centre is higher than that obtained for T7651 in the same position, practically maintaining the same texture intensity in the area close to the surface for both treatments according to Fig. 10. This means that the rolling texture is stronger for the centre of TTB than for the centre of T7651. As a consequence, there should be a higher Taylor factor ratio between the centre and the surface for the TTB sample than for the T7651 sample. Both ratios for both the T7651 heat treatment and TTB heat treatment are close to the 15% reported in [24].

4. Conclusions

From the study of the gradient of yield strength and tensile strength through the plate thickness of the RD direction in a 7449 aluminium alloy under any temper condition and its relationship with the microstructure, the following conclusions can be drawn.

1. The metallographic section of the samples in the received state in the RD direction shows much finer elongated grains in the region near the surface of the plate than in the middle. In addition, an incipient recrystallisation is observed just in the metallographic section of the area close to the surface.
2. For all heat treatments, it has been proven that the yield strength and tensile strength values vary by plate thickness, showing an increase from the surface to the centre. The largest difference has been found for the TTA sample (natural ageing).
3. The variation in Vickers hardness through the thickness of the plate is opposite to that of the variation of tensile

properties, decreasing from the surface to the centre of the plate.

4. Of all the heat treatment studied, the material in TTB condition is the one that presents the best strength-gradient relationship of the tensile properties through the thickness.
5. The orientation image maps obtained by the EBSD technique, made on the surface and in the centre of the plate, have shown that the recrystallisation process started in the area close to the surface, according to that observed by metallography. In addition, as a result of the start of the aforementioned process, the texture is much less pronounced on the surface than in the centre.
6. The gradient of the crystallography texture on the plate explains the variation of the yield strength, as the rate of change of the Taylor factor through the thickness correlates with the rate of the change of yield strength in the longitudinal direction for the samples studied.

Acknowledgments

The authors gratefully acknowledge Dr. Jose Maria Badia and Mr. Arturo Sanchez for their contribution to this work

Funding

Open Access funding provided thanks to the CRUE-CSIC agreement with Springer Nature.

Open Access

Data Availability

The raw data necessary to reproduce these conclusions are fully available.

References

1. Metallic Material Properties Development and Standardization: MMPDS-10 April 2015 7449
2. T. Dursun and C. Soutis, Recent developments in advanced aircraft aluminium alloys, *Mater. Design (1980-2015)*, 2014, **56**, p 862–871. https://doi.org/10.1016/j.matdes.2013.12.002
3. N. Kamp, I. Sinclair, and M.J. Starink, Toughness-strength relations in the overaged 7449 Al-based alloy, *Metall. Mater. Trans. A*, 2002, **33**, p 1125–1136. https://doi.org/10.1007/s11661-002-0214-2
4. J.S. Robinson and G. Higgins, The influence of quenching and ageing on fracture toughness of the Al-Zn-Mg-Cu alloy 7449, *Mater. Perform. Charact.*, 2014, **3**(3), p 370–388. https://doi.org/10.1520/mpc20130094
5. P. Schloth, A. Deschamps, C.A. Gandin, and J.M. Drezet, Modeling of GP(I) zone formation during quench in an industrial AA7449 75mm thick plate, *Mater. Des.*, 2016, **112**, p 46–57. https://doi.org/10.1016/j.matdes.2016.09.052
6. D.J. Chakrabarti, H. Weiland, B.A. Cheney, and J.T. Staley, Through thickness property variations in 7050 plate, *Mater. Sci. Forum*, 1996, **217**, p 1085–1090. https://doi.org/10.4028/www.scientific.net/msf.217-222.1085
7. J.Z. Chen, L. Zhen, B.Y. Zhang, Y.X. Cui, and S.L. Dai, Through-thickness microstructure, texture and strength gradients in AA 7055 rolled plate, *Mater. Sci. Forum*, 2007 https://doi.org/10.4028/www.scientific.net/msf.546-549.95
8. C. Li, H. Wang, W. Wang, C. Ye, Z. Jin, X. Zhang et al., Effect of solution treatment on recrystallization, texture and mechanical properties of 7A65-T74 aluminum alloy super-thick hot rolled plate, *J Wuhan Univ Technol Mater Sci Edit*, 2022, **37**(3), p 460–469. https://doi.org/10.1007/s11595-022-2552-9
9. H. Wang, Z.J. Zhang, F.G. Cong, W.C. Ren, B.S. Gong, R. Liu et al., Research on anisotropy of the 7B50 super thick plate, *J. Alloys Compd.*, 2023, **960**, p 1–16. https://doi.org/10.1016/j.jallcom.2023.171004
10. A.K. Vasudévan, W.G. Fricke, R.C. Malcolm, R.J. Bucci, M.A. Przystupa, and F. Barlat, On through thickness crystallographic texture gradient in Al-Li-Cu-Zr alloy, *Metall. Trans. A*, 1988, **19**(3), p 731–732. https://doi.org/10.1007/BF02649289
11. M. Salazar-Guapuriche, Y.Y. Zhao, A. Pitman, and A. Greene, Variations of properties across plate thickness for Al alloy 7010, *Trans. Nonferrous Met. Soc. China*, 2005, **15**(6), p 1258–1263.
12. N. Chobaut, J. Repper, T. Pirling, D. Carron, and J.-M. Drezet, Residual stress analysis in AA7449 as-quenched thick plates using neutrons and Fe modelling, in *ICAA13 Pittsburgh. Proceedings of the 13th International Conference on Aluminum Alloys*, (Springer International Publishing, 2012), pp. 285–291. https://doi.org/10.1007/978-3-319-48761-8_44
13. J.S. Robinson, S. Hossain, C.E. Truman, A.M. Paradowska, D.J. Hughes, R.C. Wimpory, and M.E. Fox, Residual stress in 7449 aluminium alloy forgings, *Mater. Sci. Eng. A*, 2010, **527**(10–11), p 2603–2612. https://doi.org/10.1016/j.msea.2009.12.022
14. J.E. Hatch Ed., *Aluminum: Properties and Physical Metallurgy*, ASM International, Aluminum Association, Detroit, 1984
15. UNE-EN-ISO 6892-1:2009. Materiales metálicos. Ensayo de tracción. Parte 1: Método de ensayo a temperatura ambiente (in Spanish)
16. G. Fribourg, Precipitation and plasticity couplings in a 7xxx aluminium alloy: application to thermomechanical treatments for distortion correction of aerospace component (Doctoral dissertation, Institute National Polytechnique of Grenoble- INPG) (2009)
17. J.R. David Ed., *ASM Specialty Handbook, Aluminium and Aluminium Alloy*, ASM International, Detroit, 1993
18. A. Brotzu, G. De Lellis, F. Felli, and D. Pilone, Study of defect formation in Al 7050 alloys, *Procedia Struct. Integr.*, 2017, **3**, p 246–252. https://doi.org/10.1016/j.prostr.2017.04.015
19. P.A. Rometsch, Y. Zhang, and S. Knight, Heat treatment of 7xxx series aluminium alloys—some recent developments, *Trans. Nonferrous Met. Soc. China*, 2014, **24**(7), p 2003–2017. https://doi.org/10.1016/S1003-6326(14)63306-9
20. D.K. Xu, P.A. Rometsch, and N. Birbilis, Improved solution treatment for and as-rolled Al-Zn-Mg-Cu alloy. Part I. Characterisation of constituent particles and overheating, *Mater. Sci. Eng. A*, 2012, **534**, p 234–243. https://doi.org/10.1016/j.msea.2011.11.065
21. D.K. Xu, P.A. Rometsch, and N. Birbilis, Improved solution treatment for an as-rolled Al-Zn-Mg-Cu alloy. Part II. Microstructure and mechanical properties, *Mater. Sci. Eng. A*, 2012, **534**, p 244–252. https://doi.org/10.1016/j.msea.2011.11.073
22. N.M. Han, X.M. Zhang, S.D. Liu, D.G. He, and R. Zhang, Effect of solution treatment on the strength and fracture toughness of aluminium alloy 7050, *J. Alloy. Compd.*, 2011, **509**(10), p 4138–4145. https://doi.org/10.1016/j.jallcom.2011.01.005
23. D. Dumont, A. Deschamps, and Y. Brechet, On the relationship between microstructure, strength, and toughness in AA 7050 alu-

minium alloy, *Mater. Sci. Eng. A*, 2003, **356**(1–2), p 326–336. https://doi.org/10.1016/S0921-5093(03)00145-X
24. M.J. Starink and S.C. Wang, A model for the yield strength of overaged Al-Zn-Mg-Cu alloys, *Acta Mater.*, 2003, **51**(17), p 5131–5150. https://doi.org/10.1016/S1359-6454(03)00363-X